Atmos. Meas. Tech. Discuss., 7, 6501–6528, 2014
www.atmos-meas-tech-discuss.net/7/6501/2014/
doi:10.5194/amtd-7-6501-2014

Atmospheric Measurement Techniques Discussions
Open Access

First measurements of continuous $\delta^{18}O$-CO_2 with a Fourier Transform InfraRed spectrometer in Heidelberg, Germany

S. N. Vardag[1], S. Hammer[1], M. Sabasch[1], D. W. T. Griffith[2], and I. Levin[1]

[1]Institut für Umweltphysik, Heidelberg University, Heidelberg, Germany
[2]Department of Chemistry, University of Wollongong, Wollongong, Australia

Received: 15 May 2014 – Accepted: 23 June 2014 – Published: 3 July 2014

Correspondence to: S. N. Vardag (svardag@iup.uni-heidelberg.de)

Published by Copernicus Publications on behalf of the European Geosciences Union.

Abstract

The continuous in-situ measurement of $\delta^{18}O$ in atmospheric CO_2 opens a new door to differentiating between CO_2 source and sink components with high temporal resolution. Continuous ^{13}C-CO_2 measurement systems have been commercially available already for some time, but until now, only few instruments have been able to provide a continuous measurement of the oxygen isotope ratio in CO_2. Besides precise $^{13}C/^{12}C$ observations, the Fourier Transform InfraRed (FTIR) spectrometer also measures the $^{18}O/^{16}O$ ratio of CO_2, but the precision and accuracy of the measurements has not been evaluated yet. Here we present a first analysis of $\delta^{18}O$-CO_2 (and $\delta^{13}C$-CO_2) measurements with the FTIR in Heidelberg. We find that our spectrometer measures ^{18}O in CO_2 with a reproducibility of better than 0.3 ‰ at a temporal resolution of less than 10 min, as determined from surveillance gas measurements over a period of ten months. An Allan deviation test shows that the $\delta^{18}O$ repeatability reaches 0.15 ‰ for half-hourly means. The compatibility of our spectroscopic measurements was determined by comparing FTIR measurements of calibration gases and ambient air to mass-spectrometric measurements of flask samples, filled with the cylinder gases or episodically collected over a diurnal cycle (event). We found that direct cylinder gas measurements agree to 0.01 ± 0.04 ‰ (mean and standard deviation) for $\delta^{13}C$-CO_2 and 0.01 ± 0.11 ‰ for $\delta^{18}O$. Two weekly episodes of recent ambient air measurements, one in winter and one in summer, are discussed in view of the question, which potential insights and new challenges combined highly resolved $\delta^{18}O$-CO_2 and $\delta^{13}C$-CO_2 records may provide in terms of better understanding regional scale continental carbon exchange processes.

1 Introduction

In order to study the impact and fate of increasing anthropogenic CO_2 emissions to the atmosphere, quantitative understanding of the processes in the carbon cycle is

AMTD
7, 6501–6528, 2014

vital. The interaction between atmosphere, biosphere and ocean must be studied in all its complexity. The stable isotopes in CO_2 can provide information about the fluxes between the different carbon reservoirs. $^{13}CO_2$ measurements can be used to distinguish between terrestrial biosphere and marine fluxes (Keeling et al., 1989; Ciais et al., 1995), and are also used as tracer for anthropogenic emissions, as most fossil fuel CO_2 emissions are depleted in ^{13}C relative to those of the biosphere (Tans, 1981). The interpretation of atmospheric $\delta^{18}O$-CO_2 is more complex since the ^{18}O-CO_2 cycle is strongly coupled to the water cycle (e.g. Francey and Tans, 1987; Farquhar et al., 1993; Cuntz et al., 2003a, b). During CO_2 exchange with soil and leaves, the ^{18}O isotopes of CO_2 are exchanged with those of H_2O (Hesterberg and Siegenthaler, 1991). The equilibration with leaf water is facilitated by carbonic anhydrase (Gillon and Yakir, 2001). The isotopic composition of soil water is determined by the isotopic composition of precipitation, which itself has strong spatial variations (IAEA/WMO GNIP database available at http://isohis.iaea.org). Since precipitation at higher latitudes is depleted in ^{18}O, the CO_2 from root respiration and heterotrophic respiration is depleted in ^{18}O too (Farquhar et al., 1993), but due to ^{18}O enrichment during evapotranspiration, the plant leaf water is enriched in ^{18}O relative to the soil water (Farquhar et al., 1993). During photosynthesis, CO_2 equilibrates with enriched leaf water and about 2/3 of the CO_2 retro-diffuses into the atmosphere without being assimilated (Tans, 1998) and therewith enriches the atmospheric $\delta^{18}O$-CO_2 value. Also diffusion into and out of the soil may change the atmospheric oxygen isotopic composition (Tans, 1998). Therefore, in order to understand and use the $\delta^{18}O$-CO_2 measurements, information about the regional isotopic composition of precipitation, as well as environmental parameters such as temperature and water vapour deficit are important (Ciais et al., 1997; Cuntz et al., 2003a). Only then, it will become possible to understand the ^{18}O-CO_2 fluxes i.e. from and to the terrestrial biosphere (Yakir and Wang, 1996; Langendörfer et al., 2002).

In order to achieve continuous estimates of the two-way gross biogenic fluxes, continuous isotopic data are necessary. However, respective measurements via mass spectrometry are elaborate and time-consuming, which is why not many continuous records

AMTD
7, 6501–6528, 2014

of ^{18}O in CO_2 exist so far (Flanagan et al., 1997; Bowling et al., 2003; Pataki et al., 2003). Quantum cascade laser-based absorption spectrometer measure $^{12}C^{16}O^{18}O$ with a high temporal resolution and provided first continuous records (Tuszon et al., 2011; Sturm et al., 2013). In principle, an in-situ Fourier Transform Infrared (FTIR) spectrometer could also allow to obtain a continuous data set of $^{12}C^{16}O^{18}O$. The FTIR spectrometer uses molecular absorption in the infrared to analyze the amount of trace gases in an air sample (Griffith et al., 2000). Since the $^{12}C^{16}O^{18}O$ isotopologue absorbs in the infrared as well, it is in principle possible to analyse also the $^{18}O/^{16}O$ ratio in CO_2. However, in their description of the instrument Esler et al. (2000) have remarked that the degree of precision is too poor for a useful determination in natural abundances using a 1 cm^{-1} resolution spectrometer. The precision of $\delta^{18}O$ measurements actually achieved has, however, not been stated in Esler et al. (2000). The reason for the difficulty of resolving $^{12}C^{16}O^{18}O$ lies in the weak absorption of $^{12}C^{16}O^{18}O$ in the infrared, which overlaps with the absorption band of the more abundant molecule $^{12}C^{16}O_2$ (see Fig. 1). Careful analysis is required to distinguish between both of them unambiguously with sufficient accuracy and precision.

Here we provide a first assessment of the $\delta^{18}O$-CO_2 (and $\delta^{13}C$-CO_2) measurements obtained with the Heidelberg FTIR instrument in terms of precision and accuracy. Continuous atmospheric data are compared to conventional mass spectrometric observations to investigate the uncertainty of these measurements. Finally first applications of the highly resolved $\delta^{18}O$-CO_2 record (along with the continuous CO_2, CO and $\delta^{13}C$-CO_2 records) are discussed and the question is investigated which insight into regional scale carbon exchange processes may be gained through these isotopologue records.

2 FTIR measurement principle and calibration procedure

The in-situ FTIR used in Heidelberg has been developed at the University of Wollongong, Australia (Griffith et al., 2012). Details concerning the Heidelberg set-up of the spectrometer can be found in Hammer et al. (2013). Basically, the FTIR obtains

AMTD
7, 6501–6528, 2014

a transmittance spectrum by taking the ratio of the infrared spectra measured with and without a sample in the optical cell. The transmittance spectrum is then evaluated with a fitting algorithm called MALT (Multi-Layer Absorption Transmittance), which generates a theoretical transmittance spectrum for gas samples with different gas compositions. This is described in more detail by Griffith (1996) and Griffith et al. (2012). The generated theoretical spectrum is compared to the measured spectrum, and the residual of this comparison is minimised by a non-linear least squares fitting algorithm, varying the trace gas composition and instrument parameters in the theoretical spectrum. The raw trace gas concentration can then be derived.

2.1 Data evaluation and calibration

In the following, the data evaluation and calibration procedure is described for the isotopologue ratio δ^{18}O-CO_2, but it is done in an analogous way for δ^{13}C-CO_2.

Step 1: calculate the raw δ^{18}O value from FTIR measurements

The FTIR computes the raw δ^{18}O value as the ratio of the raw value of the rare isotopologue and the raw value of the common isotopologue:

$$\text{Molec} - \delta^{18}\text{O}_{\text{HITRAN}} - \text{CO}_2 = [(^{12}\text{C}^{18}\text{O}^{16}\text{O}_{\text{raw}}/^{12}\text{C}^{16}\text{O}^{16}\text{O}_{\text{raw}})_{\text{sample}}/R_{\text{HITRAN}} - 1] \times 1000‰ \quad (1)$$

with $R_{\text{HITRAN}} = 0.00401126$.

Note that we here use the expression "Molec-δ^{18}O" since commonly the δ-notation is defined with isotope ratios rather than isotopologue ratios. The FTIR implicitly uses the HITRAN scale (Rothman et al., 2005), which is referred to VPDB for δ^{13}C and to VSMOW for δ^{18}O; but during the calibration (step 3) the final reference scale of the calibrated data can be changed to any other scale. From now on, we chose VPDB-CO_2 for δ^{18}O and VPDB for δ^{13}C. We abbreviate δ^{18}O-CO_2 on the VPDB-CO_2 scale with $\delta^{18}\text{O}_{\text{VPDB}}$ and δ^{13}C-CO_2 on the VPDB scale with $\delta^{13}\text{C}_{\text{VPDB}}$.

AMTD
7, 6501–6528, 2014

Step 2: cross-sensitivity and inter-species interference corrections

Even though the software MALT takes into account influences from pressure, temperature and inter-species overlapping absorption bands, residual sensitivity corrections of certain parameters and species need to be performed (see Hammer et al., 2013). A cross-sensitivity correction for sample temperature and pressure, H_2O abundance and flow rate, as well as an interspecies-sensitivity correction for CO_2 mole fraction is done for every measurement. The sensitivity of Molec-δ^{18}O-CO_2 and Molec-δ^{13}C-CO_2 to CO_2 are shown in Fig. 2. The set-up of the experiment to determine this sensitivity is described in detail by Hammer et al. (2013). A cubic fit is used to describe the CO_2 interspecies correction. The residual sum of squares between the measurement and the cubic fit divided by the number of measurements is ±0.001 ‰ for δ^{13}C and ±0.041 ‰ for δ^{18}O with residuals showing no further concentration dependence (Fig. 2b and d).

Step 3: calibration

The cross-sensitivity corrected data is calibrated on the VPDB gas scale using a linear instrument response function (typically linear to the degree of $R = 0.9999$). The calibration (response function) is derived from three reference tanks with known values for CO_2, δ^{13}C-CO_2 and δ^{18}O-CO_2. This response function is determined weekly. Our reference standards span ranges from about 370 µmol mol^{-1} to 470 µmol mol^{-1} for CO_2 mole fraction, a $\delta^{13}C_{VPDB}$ range from −8.7 ‰ to −12.8 ‰ and a $\delta^{18}O_{VPDB}$ range from −1.9 ‰ to −5.0 ‰ (as determined by the Heidelberg mass spectrometer (MS)). For details on the MS, see Neubert (1998).

Step 4: smoothed working standard correction

We have found that the measurement of different cylinder gases on the FTIR show very similar sub-weekly variations of δ^{18}O-CO_2. One can thus use a smoothed working standard correction in order to account for these small instrumental variations

AMTD
7, 6501–6528, 2014

on a sub-weekly time scale. For this purpose, daily working gas measurements are smoothed and the smoothed residual variations from the long-term mean value of this gas vs. the reference standards are subtracted from all measurements. By performing this correction, the standard deviation of a weekly measured target or surveillance gas reaches about 0.2 ‰. Step 4 is not obligatory, but could further increase the precision of the measurement. In the data presented in Sect. 4 we have applied a smoothed working standard correction.

Figure 3 illustrates the application of the calibration procedure. For δ^{13}C, Fig. 3 shows raw (a), corrected (b) and calibrated (c) FTIR measurements against MS reference values of δ^{13}C respectively, and Fig. 3d shows the difference between calibrated FTIR measurements and MS values (FTIR-MS) against CO_2 mole fractions. Figure 3e–h show corresponding data for δ^{18}O. The cross-sensitivity correction forces Molec-δ^{13}C and Molec-δ^{18}O on a linear regression line (Fig. 3b and f), so that a linear calibration can then be applied.

2.2 Remarks on the calibration procedure

2.2.1 Using CO_{2total} instead of $^{12}C^{16}O_2$ in Eq. (1)

Total raw CO_2 mole fraction is retrieved from absorption bands near 3600 cm^{-1}. $^{12}CO_2$, $^{13}CO_2$ as well as $^{12}C^{16}O^{18}O$ absorb in this region but the minor isotopologue absorptions are weak and are hardly distinguishable. In the stronger absorption band near 2300 cm^{-1} (see Fig. 1) the CO_2 isotopologues have distinguishable absorption regions and structures and can therefore be obtained individually. The precision of total CO_2 in the 3600 cm^{-1} range is, however, about 50 % higher than that of $^{12}CO_2$ in the region of 2300 cm^{-1}, due to an optimum absorption and a lower temperature sensitivity. Therefore, the raw Molec-δ^{18}O and Molec-δ^{13}C values are calculated using total CO_2, instead of $^{12}CO_2$. As long as the isotopic composition of the sample is close to the isotopic composition of the reference standards, the bias in δ^{18}O and δ^{13}C is negligible

AMTD
7, 6501–6528, 2014

(< 0.03 ‰ for $\delta^{13}C$ and < 0.05 ‰ for $\delta^{18}O$) after calibration (step 3). For much depleted cylinder gases, as may be the case for synthetic gas mixtures, the biases may, however, become as large as 0.2 ‰.

2.2.2 Absolute calibration

The described method of calibration (step 3) is an empirical one (Griffith et al., 2012). In principle, it is equally valid to use the "absolute calibration method". In this case, the isotopologues $^{16}O^{12}C^{16}O$, $^{16}O^{13}C^{16}O$ and $^{16}O^{12}C^{18}O$ are corrected (step 2) and calibrated (step 3) individually and finally $\delta^{18}O$ and $\delta^{13}C$ are computed from the calibrated isotopologues, i.e.

$$\delta^{18}O_{VPDB} = \left[(^{12}C^{18}O^{16}O/^{12}C^{16}O_2)_{sample}/(C^{18}O^{16}O/^{12}C^{16}O_2)_{VPDB-CO_2} - 1\right] \times 1000‰ \quad (2)$$

with $(^{12}C^{18}O^{16}O/^{12}C^{16}O_2)_{VPDB-CO_2} = 0.0041767$ (Allison et al., 1995), which takes into account that CO_2 contains two oxygen atoms. In Sect. 5, we will briefly discuss possible advantages or disadvantages of both methods.

2.3 Direct cylinder comparison to mass spectrometric values

In order to check the calibration as well as the compatibility of the FTIR and the Heidelberg mass spectrometer (MS), different test cylinders were measured in March and April 2014 on both instruments and values were compared. The Heidelberg mass spectrometric values are linked to the VPDB scale via three pure CO_2 reference gases (RM8562, RM8563, RM8564). The FTIR reference cylinders were calibrated by the Heidelberg mass spectrometer (MS) and thus the FTIR and the MS are on the same scale. For all cylinder measurements with the mass spectrometer, cylinder air was filled into evacuated flasks, which were analysed like regular flask samples, since pressure regulator effects often disturb the MS analyses.

AMTD
7, 6501–6528, 2014

3 Characterization of δ^{18}O-CO_2 and δ^{13}C-CO_2 measurements with the Heidelberg FTIR

3.1 Allan deviation

An Allan deviation test was performed on the FTIR system on the 5/6 August 2013 with a reference gas cylinder with a δ^{13}C value of -9.96 ± 0.07 ‰ and a δ^{18}O value of -1.24 ± 0.25 ‰. The Allan deviation will be used as a measure for the repeatability. It can be seen in Fig. 4a and b that the Allan deviations after a three minute measurement are about δ^{13}C = ±0.05 ‰ and δ^{18}O = ±0.45 ‰. After 10 min, they decrease to δ^{13}C = ±0.025 ‰ and δ^{18}O = ±0.25 ‰ and after 30 min, the Allan deviation reaches δ^{13}C = ±0.015 ‰ and δ^{18}O = ±0.15 ‰. In Heidelberg, a typical diurnal variation of δ^{18}O-CO_2 is in the order of 1 ‰; after about 30 min integration time the repeatability is thus typically 15 % of this diurnal signal and should therefore be good enough to significantly distinguish ambient δ^{18}O-CO_2 signals (see Sect. 4 and Fig. 7).

3.2 Reproducibility

The reproducibility can be estimated and monitored by measuring standard gases every day or week under reproducible conditions. The averaging time for cylinder measurements is 9 min. The standard deviation of the measured gases is a good measure of estimating the reproducibility of our measurements. For δ^{18}O-CO_2, the daily working cylinder reproducibility was found to be 0.27 ‰ for the period from December 2012 to October 2013. The reproducibility for δ^{13}C-CO_2 was 0.04 ‰ (see Fig. 5a and b). Thus, the reproducibility is dominated by the repeatability, suggesting a very good long-term stability of the instrumental setup. The reproducibility of the δ^{18}O-CO_2 measurements is much (ca. 1/5th) smaller than the diurnal ambient air variability, at least for the measurement site in Heidelberg (see Fig. 7).

Note that in our calibration procedure we now use the daily measured cylinder (working gas) in a final correction step (step 4) to account for sub-weekly variations of the

AMTD
7, 6501–6528, 2014

instrument response. Since we only recognized the need to correct for this variability well after commence of the measurements, we do not yet have a long-term record for a real target. Therefore, Fig. 5 displays the working standard measurements without any sub-weekly smoothing applied, which is an upper estimate of the reproducibility of real measurements where step 4 of our calibration procedure is applied in addition.

3.3 Compatibility of ambient air measurements

We have shown in Sect. 2.3 that the FTIR measures cylinders with high compatibility to the Heidelberg mass spectrometer. In order to show that there is no bias introduced when measuring ambient air, a so-called diurnal cycle "event" was evaluated. An automated flask sampler (Neubert et al., 2004) collected and dried (dew point −40 °C) ambient air from the same intake line as the FTIR into 2 L glass flasks. Every flask was flushed for two hours and then pressurized to 2 bar absolute pressure and closed. Then the next flask was opened, flushed and filled to 2 bar. Pressurizing the flasks takes about 5 min. With this procedure, a diurnal isotopic profile with a two-hourly resolution could be captured in the flasks and analyzed by mass spectrometry. These values were then compared to the nine-minutely averaged values from the FTIR spectrometer (see Fig. 6). The averaging was made to account for atmospheric variability and a possible time asynchrony between the event sampler and the FTIR, but also to reduce the noise on the FTIR measurement.

δ^{18}O agrees well within its measurement uncertainty. The mean residual and standard error for δ^{18}O is 0.08 ± 0.14 ‰, which shows that the FTIR succeeds in measuring ^{18}O in CO_2 with good accuracy. Thus, a high compatibility of the ^{18}O isotope measurements of better than 0.1 ‰ can be confirmed. The larger discrepancy (and variability) in δ^{18}O than in direct cylinder gas comparisons (Sect. 2.3) reflects the fact that there are more components contributing to the difference between the FTIR and the MS value, such as the flasks itself, which could be slightly wet and then change the δ^{18}O value of the CO_2, or some other possible interference of the automated flask sampler. For δ^{13}C, the mean residual is 0.01 ± 0.02 ‰.

AMTD
7, 6501–6528, 2014

4 Example period of continuous trace gas and stable isotopologue measurements in Heidelberg

In this section, we will give a short prospect on how to potentially use a highly resolved δ^{18}O-CO_2 record in an area such as Heidelberg in order to disentangle regional scale carbon exchange processes. For this purpose, we look at two very different periods in which the FTIR measured δ^{18}O along with δ^{13}C in CO_2, total CO_2 and CO in Heidelberg (see Fig. 7).

In order to interpret the atmospheric δ^{18}O-CO_2 variation, the isotopic signature of the processes influencing the isotopic content must be known. In the Heidelberg catchment area, the most important CO_2 fluxes are associated with plant photosynthesis, leaf and soil respiration as well as fossil fuel burning. Discrimination during photosynthesis tends to enrich atmospheric CO_2 with respect to ^{18}O and ^{13}C. Typical mean δ^{13}C fractionation relative to the atmosphere during photosynthesis is about – (2–8) ‰ for C4 plants and about – (12–20) ‰ for C3 plants (Mook, 1994). During respiration, at first approximation, the $^{13}CO_2/^{12}CO_2$ ratio captured during photosynthesis is also released, which leads to a depletion of the atmospheric $^{13}CO_2/^{12}CO_2$ ratio. In addition, ^{18}O discrimination during respiration tends to deplete the atmosphere in its δ^{18}O-CO_2 value. Due to fast equilibration with the water reservoirs, the isotopic ^{18}O signature of soil respired, leaf respired and back-diffused CO_2 during photosynthesis changes the original ^{18}O signature of the CO_2. Neubert (1998) measured the isotopic composition of soil respired CO_2 in the surroundings of Heidelberg and found values of $\delta^{18}O_{VPDB} \approx -10$ ‰ with a tendency of slightly more depleted values in the winter (−15 ‰) than in summer (−5 ‰) and $\delta^{13}C_{VPDB} \approx -25$ ‰. For the discrimination during photosynthesis, typical mean values for the Northern European continent are between 0 and 20 ‰ for ^{18}O (Farquhar et al., 1993; Cuntz et al., 2003b).

Further, the δ^{18}O source signature will be influenced also by the invasion flux (Tans, 1998; Miller et al., 1999), which occurs when CO_2 diffuses into the soil, partially equilibrates with soil water and retro-diffuses into the atmosphere. Seibt et al. (2006) have

AMTD
7, 6501–6528, 2014

shown that invasion fluxes can lead to more depleted apparent δ^{18}O soil respiration source signatures in presence of carbonic anhydrase. However Wingate et al. (2008) found more enriched apparent δ^{18}O soil respiration source signatures in presence of carbonic anhydrase. Miller et al. (1999) found that in most settings and especially in dry ground and for short residence times (corresponding to high boundary layer mixing heights), the effect will be rather small (< 5 ‰). The magnitude of this effect for our catchment area cannot be quantified without intensive sampling and isotopic soil flux modelling and thus, it will only be considered in a sense that a larger uncertainty must be attributed to the soil respiration flux. For the isotopic signature of fossil fuels, a common δ^{18}O fossil fuel signature of $\delta^{18}O_{VPDB} \approx -17$ ‰ is assumed in most studies, corresponding to the ambient oxygen isotopic signature, but incomplete combustion can lead to a range of different isotopic signatures. The ^{18}O signature of fossil fuel emissions varies from about −11 ‰ to −40 ‰ (Schumacher et al., 2011). Traffic exhausts tend to be less depleted in ^{18}O relative to other fossil fuel CO_2 emissions (ca. $\delta^{18}O_{VPDB} \approx -15$ ‰), followed by natural gas emissions ($\delta^{18}O_{VPDB} \approx -28$ ‰). Combustion of coal, on the other hand, leads to a δ^{18}O value of about −38 ‰. To our knowledge, the uncertainties of these values are not well known. For $\delta^{13}C_{VPDB}$, typical signatures are ca. −29 ‰ for traffic exhausts, −25 ‰ for coal combustion and −39 ‰ for natural gas emissions (Widory and Javoy, 2003; Kaul, 2007). With these landmarks of isotopic signatures, we can now look at the Heidelberg atmospheric CO_2 records that show values around $\delta^{18}O_{VPDB}$ of −2 ‰ to −4 ‰ in winter and 0 ‰ to −2 ‰ in summer while δ^{13}C-CO_2 varies between −8 ‰ and −12 ‰ (Fig. 7).

Since all CO_2 sources with a negative isotopic signature compared to atmospheric CO_2 lead to δ^{13}C-CO_2 or δ^{18}O-CO_2 depletion, a differentiation between different depleting sources is difficult. Therefore we used the following approach: we first constructed an artificial δ^{13}C-CO_2 and δ^{18}O-CO_2 record using the slope and offset of so called "Keeling plots" (Keeling, 1958) determined from measured values in an exemplary and short night time reference period (ref) (gray bars in Fig. 7) according to:

AMTD
7, 6501–6528, 2014

$$\delta_{meas}(ref) = slope(ref) \times 1/CO_2(ref) + offset(ref) \quad (3)$$

Note that in the nighttime reference periods, for which the reference slope and offsets were calculated, we can neglect any photosynthetic sinks. Therefore, the $\delta^{13}C$ source signature of the reference period can be interpreted as the flux-weighted average of all sources (Miller and Tans, 2003). We then applied the parameters from the reference period to the entire CO_2 record to calculate artificially constructed $\delta^{13}C_{constr}$ and $\delta^{18}O_{constr}$ values over time (t).

$$\delta_{constr}(t) = slope(ref) \times 1/CO_{2,meas}(t) + offset(ref) \quad (4)$$

The constructed $\delta^{13}C$ and $\delta^{18}O$ records are shown in burgundy and light blue in Fig. 7a, b, g and h. During the reference period, in which the Keeling plot slopes and offsets were derived, the Keeling plot had a high correlation ($r^2 > 0.85$) and showed an isotopic ^{13}C and ^{18}O signature, which was typical for the respective season ($\delta^{13}C$-$CO_2 \approx -25$ ‰ in the winter and -27 ‰ in the summer period, $\delta^{18}O$-$CO_2 \approx -28$ ‰ in the winter and -12 ‰ in the summer period). To identify enriching or depleting sources and sinks relative to the reference period, we then calculated the difference between the real measured and the artificially constructed (Eq. 4) $\delta^{13}C$ and $\delta^{18}O$ record (Fig. 7e, k, f and l).

$$\Delta\delta(t) = \delta_{meas}(t) - \delta_{constr}(t). \quad (5)$$

Negative $\Delta\delta$ values occur in periods when the apparent sources are more depleted than in the reference period and positive values occur when apparent sources are more enriched than in the reference period. During photosynthetic CO_2 uptake the equilibration of back-diffusing CO_2 with enriched leaf water leads to an enrichment of atmospheric $\delta^{18}O$ and thus to positive $\Delta\delta^{18}O$ values. We, thus, now have a tool at hand, which allows differentiating between more and less depleted fluxes relative to the reference period.

AMTD
7, 6501–6528, 2014

In the wintertime, relative fossil fuel contributions in the Heidelberg catchment area are higher than in the summer time (Levin et al., 2003). Fossil fuel CO_2 emissions lead to high concentration of CO_2 (Fig. 7d) and deplete atmospheric CO_2 in its heavy isotopes ^{13}C and ^{18}O (original measurements: dark blue and red in Fig. 7a and b). During incomplete combustion of fossil fuels, CO (Fig. 7c) is often emitted as well. A typical example of a pollution event can be seen in Fig. 7 (left panel) on 21 December 2012. The difference between the measured and artificially constructed $\delta^{13}C$ (Fig. 7e) decreases rapidly on the 21 December, indicating a source (mix) which is more depleted in ^{13}C than during the reference period ($\delta^{13}C_{ref} = -25$ ‰). The strong influence of a more ^{13}C depleted source mix points towards a high contribution from fossil fuel sources, including domestic heating (natural gas). At the same time the isotopic signature of $\delta^{18}O$ is very close to the isotopic signature during the reference period (−28 ‰) and increases during the pollution event. The different behavior of $\delta^{13}C$ and $\delta^{18}O$ in CO_2 points towards a larger influence from traffic or natural gas combustion, as both sources are slightly more enriched in ^{18}O, but less enriched in ^{13}C with respect to coal-fired combustion (Schumacher et al., 2011). One can see that the fact that different fossil fuel types influence both stable isotopes ^{13}C and ^{18}O in CO_2 in a different way can be used to differentiate between different emission groups in situations when biogenic fluxes are low (i.e. in winter). However, for a quantitative analysis the exact isotopic signatures of all fluxes in the area of influence must be known.

In the summer time, we expect biosphere fluxes to be much larger than during winter and at the same time fossil fuel (especially residential heating) emissions to be smaller than in winter. In fact, we do not find large deviations in $\delta^{13}CO_2$ from those determined in the reference period (−27 ‰), pointing towards a relatively constant mixture of biogenic and fossil fuel emissions. On the other hand, the measured $\delta^{18}O$ decreases rapidly on the 3 July compared to the reference period with a source isotopic signature of ≈ −12 ‰. This decrease is not accompanied with changes of any other tracer, such as CO, $\delta^{13}CO_2$ or CO_2. A possible explanation for the decrease is a change in the hydrological conditions. After four dry days, a sudden heavy rain occurred in Heidelberg

AMTD
7, 6501–6528, 2014

on the 3 July (see dashed bar in Fig. 7, right panel). The rainfall replenished the water reservoirs and a new equilibrium value between the soil and leaf water reservoirs and CO_2 most probably caused the atmospheric δ^{18}O-CO_2 to become depleted relative to the reference period. This example shows how closely coupled δ^{18}O in the water and carbon cycle are. In order to quantitatively use the δ^{18}O-CO_2 records it is thus crucial to study also the hydrological conditions, such as precipitation and its isotopic signature.

5 Discussion

5.1 Instrumental challenges

In Sect. 2 we have described two possible evaluation and calibration methods; the absolute (Sect. 2.2.2) and the empirical method (Sect. 2.1). Even though in principle both methods should lead to the same results, they differ slightly by about 0.11 ± 0.03 ‰ for δ^{13}C (mean ± standard deviation for a two-monthly period in 2014) and by 0.08 ± 0.15 ‰ for δ^{18}O. The discrepancy between both calibration methods is most likely due to small inaccuracies in interspecies interference corrections. The empirical calibration requires a large CO_2-cross-sensitivity correction over a large CO_2 range (see Fig. 2c). Only if the CO_2 interspecies-sensitivity correction is applied with high accuracy, reliable δ^{18}O can be obtained. For the absolute calibration, no CO_2 correction is required, but a very accurate determination of all CO_2 isotopologue calibration equations is vital. Small errors in the inter-species interference corrections of the CO_2 isotopologues can lead to large errors in the δ^{13}C and δ^{18}O values. The decision on which method to use should thus be based on which correction can be performed with higher accuracy. In this work we have found for the Heidelberg spectrometer that the empirical calibration method better fits the Heidelberg mass spectrometer values.

AMTD
7, 6501–6528, 2014

5.2 Quantitative interpretation of continuous δ^{13}C and δ^{18}O record

For δ^{13}C, the different carbon sources and sinks are relatively well understood, but for δ^{18}O, high temporal and spatial variability of the respiratory and photosynthetic fluxes (due to a strong variation of environmental parameters such as temperature, humidity and geographical position) makes it difficult to separate the different CO_2 fluxes. For our qualitative study, we could use observations from Neubert (1998) in the catchment area of Heidelberg, as well as globally resolved model data for assimilation isofluxes from Cuntz et al. (2003b). However, for a quantitative apportionment of the CO_2 fluxes at a high temporal resolution, sampling of the isotopic content of precipitation, soil respiration and foliage gas exchange in the catchment area will be necessary on similarly high temporal resolution (Stern et al., 1999). Further, invasion flux models are required to quantify the effect of this process at the measurement site. All these unknowns largely limit current applicability of our new continuous isotope measurements. Only future sophisticated regional models of the water and the carbon cycle could fully exploit the wealth of new information now available.

6 Summary and conclusion

The accurate analysis of δ^{18}O in CO_2 using FTIR spectrometry is novel. The $CO^{18}O$ measurements of the FTIR in Heidelberg were evaluated with regard to long-term stability, reproducibility and accuracy. We found that the reproducibility of daily working standard gas measurements, averaged over nine minutes, is δ^{18}O = ±0.27 ‰. The Allan deviation of three-minutely δ^{18}O- measurements was determined to about ±0.45 ‰ and it decreases to ±0.15 ‰ for hourly averages. Depending on the magnitude of atmospheric variability and on the field of application, it could be worthwhile to aggregate three-minutely δ^{18}O measurements to half- or one-hourly averages. Even then, a much higher temporal resolution than provided by mass-spectrometric analyses can be achieved. Even though the FTIR precision does not reach the WMO ILC

AMTD
7, 6501–6528, 2014

targets (WMO, 2009), a number of interesting scientific applications seem possible using a FTIR. In particular, investigation of processes that govern the $\delta^{18}O$ variability of atmospheric CO_2 on the regional scale seem very promising. However, quantitative analysis requires comprehensive knowledge on the isotopic signature of different CO_2 sources and sinks as well as of the influencing water reservoirs.

Acknowledgements. This work has been funded by the InGOS EU project (284274). We further acknowledge the financial support given by Deutsche Forschungsgemeinschaft and Ruprecht-Karls-Universität Heidelberg within the funding program Open Access Publishing.

References

Allison, C., Francey, R., and Meijer, H.: Recommendations for the reporting of stable isotope measurements for carbon and oxygen in CO_2 gas, reference and intercomparison materials for stable isotopes of light element, IAEA-TECDO, 155–162, 1995.

Bowling, D. R., McDowell, N. G., Welker, J. M., Bind, B. J., Law, B. E., and Ehleringer, J. R.: Oxygen isotope content of CO_2 in nocturnal ecosystem respiration: 1. Observations in forests along a precipitation transect in Oregon, USA, Global Biogeochem. Cy., 17, 1120, doi:10.1029/2003GB002081, 2003.

Ciais, P., Tans, P. P., White, J. W. C., Trolier, M., Francey, R. J., Berry, J. A., Randall, D. R., Sellers, P. J., Collatz, J. G., and Schimel, D. S.: Partitioning of ocean and land uptake of CO_2 as inferred by $\delta^{13}C$ measurements from the NOAA Climate Monitoring and Diagnostics Laboratory Global Air Sampling Network, J. Geophys. Res., 100, 5051–5070, doi:10.1029/94JD02847, 1995.

Ciais, P. et al.: A three-dimensional synthesis study of $\delta^{18}O$ in atmospheric CO_2: 1. surface fluxes, J. Geophys. Res., 102, 5857–5872, doi:10.1029/96JD02360, 1997.

Cuntz, M., Ciais, P., Hoffmann, G., and Knorr, W.: A comprehensive global three-dimensional model of $\delta^{18}O$ in atmospheric CO_2: 1. Validation of surface processes, J. Geophys. Res., 108, 4527, doi:10.1029/2002JD003153, 2003a.

Cuntz, M., Ciais, P., Hoffmann, G., Allison, C. E., Francey, R. J., Knorr, W., Tans, P. P., White, J. W. C., and Levin, I.: A comprehensive global three-dimensional model of $\delta^{18}O$

in atmospheric CO_2: 2. Mapping the atmospheric signal, J. Geophys. Res., 108, 4528, doi:10.1029/2002JD003154, 2003b.
Esler, M. B., Griffith, D. W. T., Wilson, S. R., and Steele, L. P.: Precision trace gas analysis by FT-IR Spectroscopy, 2. The $^{13}C/^{12}C$ isotope ratio of CO_2, Anal. Chem., 72, 216–221, 2000.
Farquhar, G. D., Lloyd, J., Taylor, J. A. et al.: Vegetation effects on the isotope composition of oxygen in atmospheric CO_2, Nature, 363, 439–442, 1993.
Flanagan, L. B., Brooks, J. R., Varney, G. T., and Ehleringer, J. R.: Discrimination against $C^{18}O^{16}O$ during photosynthesis and the oxygen isotope ratio respired CO_2 in boreal forest ecosystems, Global Biogeochem. Cy., 11, 83–98, 1997.
Francey, R. J. and Tans, P. P.: Latitudinal variation in oxygen-18 of atmospheric CO_2, Nature, 327, 495–497, doi:10.1038/327495a0, 1987.
Gillon, J. and Yakir, D.: Influence of carbonic anhydrase activity in terrestrial vegetation on the ^{18}O content of atmospheric CO_2, Science, 291, 2584–2587, doi:10.1126/science.1056374, 2001.
Griffith, D. W. T.: Synthetic calibration and quantitative analysis of gas phase infrared spectra, Appl. Spectrosc., 50, 59–70, 1996.
Griffith, D. W. T. and Jamie, I. M.: Fourier transform infrared spectrometry in atmospheric and trace gas analysis, in: Encyclopedia of Analytical Chemistry, edited by: Meyers,. R. A., Wiley, Chichester, 1979–2007, 2000.
Griffith, D. W. T., Deutscher, N. M., Caldow, C., Kettlewell, G., Riggenbach, M., and Hammer, S.: A Fourier transform infrared trace gas and isotope analyser for atmospheric applications, Atmos. Meas. Tech., 5, 2481–2498, doi:10.5194/amt-5-2481-2012, 2012.
Hammer, S., Griffith, D. W. T., Konrad, G., Vardag, S., Caldow, C., and Levin, I.: Assessment of a multi-species in situ FTIR for precise atmospheric greenhouse gas observations, Atmos. Meas. Tech., 6, 1153–1170, doi:10.5194/amt-6-1153-2013, 2013.
Hesterberg, R. and Siegenthaler, U.: Production and stable isotopic composition of CO_2 in a soil near Bern, Switzerland, Tellus B, 43, 197–205, doi:10.1034/j.1600-0889.1991.00013.x, 1991.
Kaul, M.: Isotopenverhältnisse im atmosphärischem Kohlendioxid und seine Quellen im Raum Heidelberg, Staatsexamen thesis, Universität Heidelberg, 2007.
Keeling, C. D.: The concentration and isotopic abundance of atmospheric carbon dioxide in rural areas, Geochim. Cosmochim. Ac., 13, 322–334, 1958.

AMTD
7, 6501–6528, 2014

Keeling, C. D., Bacastow, R. B., Carter, A. F., Piper, S. C., Whorf, T. P., Heimann, M., Mook, W. G., and Roeloffzen, H.: A three-dimensional model of atmospheric CO_2 transport based on observed winds: 1. Analysis of observational data, in: Aspects of Climate Variability in the Pacific and the Western Americas, Vol. 55, edited by: Peterson, D. H., American Geophysical Union, Washington, DC, 165–236, 1989.

Langendörfer, U., Cuntz, M., Ciais, P., Peylin, P., Bariac, T., Milyukova, I., Kolle, O., Naegler, T., and Levin, I.: Modelling of biospheric CO_2 gross fluxes via oxygen isotopes in a spruce forest canopy: a ^{222}Rn calibrated box model approach, Tellus B, 54, 476–496, doi:10.1034/j.1600-0889.2002.01345.x, 2002.

Levin, I., Kromer, B., Schmidt, M., and Sartorius, H.: A novel approach for independent budgeting of fossil fuel CO_2 over Europe by $^{14}CO_2$ observations, Geophys. Res. Lett., 30, 2194, doi:10.1029/2003GL018477, 2003.

Miller, J. B. and Tans, P. P.: Calculating isotopic fractionation from atmospheric measurements at various scales, Tellus B, 55, 207–214, doi:10.1034/j.1600-0889.2003.00020.x, 2003.

Miller, J. B., Yakir, D., White, J. W. C., and Tans, P. P.: Measurement of $^{18}O/^{16}O$ in the soil–atmosphere CO_2 flux, Global Biogeochem. Cy., 13, 761–774, doi:10.1029/1999GB900028, 1999.

Mook, W.: Environmental Isotopes in the Hydrological Cycle – Principles and Applications, Introductory Course on Isotope Hydrology, Department of Hydrogeology and Geographical Hyrdology, 1994.

Neubert, R.: Measurement of stable isotopomers of atmospheric carbon dioxide, Ph.D. thesis, University of Heidelberg, 1998.

Neubert, R. E. M., Spijkervet, L. L., Schut, J. K., Been, H. A., and Meijer, H. A. J.: A computer-controlled continuous air drying and flask sampling system, J. Atmos. Ocean. Tech., 21, 651–659, 2004.

Pataki, D. E., Bowling, D. R., and Ehleringer, J. R.: Seasonal cycle of carbon dioxide and its isotopic composition in an urban atmosphere: anthropogenic and biogenic effects., J. Geophys. Res., 108, 4735, doi:10.1029/2003JD003865, 2003.

Rothman, L. S., Jacquemart, D., Barbe, A., Benner, D. C., Birk, M., Brown, L. R., Carleer, M. R., C. Chaucerian, J., Chance, K., Dana, V., Devi, V. M., Flaud, J.-M., Gamache, R. R., Goldman, A., Hartmann, J.-M., Jucks, K. W., Maki, A. G., Mandin, J.-Y., Massie, S. T., Orphali, J., Perrin, A., Rinsland, C. P., Smith, M. A. H., Tennyson, J.,

AMTD
7, 6501–6528, 2014

Tolchenov, R. N., Toth, R. A., Auwera, J. V., Varanasi, P., and Wagner, G.: The HITRAN 2004 molecular spectroscopic database, J. Quant. Spectrosc. Ra., 96, 139–204, 2005.
Schumacher, M., Werner, R. A., Meijer, H. A. J., Jansen, H. G., Brand, W. A., Geilmann, H., and Neubert, R. E. M.: Oxygen isotopic signature of CO_2 from combustion processes, Atmos. Chem. Phys., 11, 1473–1490, doi:10.5194/acp-11-1473-2011, 2011.
Seibt, U., Wingate, L., Lloyd, J., and Berry, J. A.: Diurnally variable $\delta^{18}O$ signatures of soil CO_2 fluxes indicate carbonic anhydrase activity in a forest soil, J. Geophys. Res., 111, G04005, doi:10.1029/2006JG000177, 2006.
Stern, L., Baidsen, W. T., and Amundson, R.: Processes controlling the oxygen isotopic ratio of soil CO_2: analytical andnumerical modelling, Geochim. Cosmochim. Ac., 63, 799–814, 1999.
Sturm, P., Tuzson, B., Henne, S., and Emmenegger, L.: Tracking isotopic signatures of CO_2 at the high altitude site Jungfraujoch with laser spectroscopy: analytical improvements and representative results, Atmos. Meas. Tech., 6, 1659–1671, doi:10.5194/amt-6-1659-2013, 2013.
Tans, P. P.: $^{13}C/^{12}C$ of industrial CO_2, carbon cycle modelling, Scope Ser., 16, 127–129, 1981.
Tans, P. P.: Oxygen isotopic equilibrium between carbon dioxide and water in soils, Tellus B, 50, 163–178, doi:10.1034/j.1600-0889.1998.t01-1-00004.x, 1998.
Tuzson, B., Henne, S., Brunner, D., Steinbacher, M., Mohn, J., Buchmann, B., and Emmenegger, L.: Continuous isotopic composition measurements of tropospheric CO_2 at Jungfraujoch (3580 m a.s.l.), Switzerland: real-time observation of regional pollution events, Atmos. Chem. Phys., 11, 1685–1696, doi:10.5194/acp-11-1685-2011, 2011.
Wendeberg, M., Richter, J. M., Rothe, M., and Brand, W. A.: Jena Reference Air Set (JRAS): a multi-point scale anchor for isotope measurements of CO_2 in air, Atmos. Meas. Tech., 6, 817–822, doi:10.5194/amt-6-817-2013, 2013.
Widory, D. and Javoy, M.: The carbon isotope composition of atmospheric CO_2 in Paris, Earth Planet. Sc. Lett., 215, 289–298, 2003.
Wingate, L., Seibt, U., Maseyk, K., Ogée, J., Almeida, P., Yakir, D., Pereira, J. S., and Menunccini, M.: Evaporation and carbonic anhydrase activity recorded in oxygen isotope signatures of net CO_2 fluxes from a Mediterranean soil, Glob. Change Biol., 14, 2178–2193, doi:10.1111/j.1365-2486.2008.01635.x, 2008.
WMO: Report of the 15th WMO/IAEA Meeting of Experts on Carbon Dioxide, Other Greenhouse Gases and Related Tracers Measurement Techniques (GGMT-2009), Jena, Germany,

AMTD
7, 6501–6528, 2014

7–10 September 2009, GAW Report No. 194, available at: http://www.wmo.int/pages/prog/arep/gaw/gaw-reports.html (last access: 17 February 2014), Jena, Germany, 2009.
Yakir, D. and Wang, X.-F.: Fluxes of CO_2 and water between terrestrial vegetation and the atmosphere estimated from isotope measurements, Letters to Nature, 380, 515–517, 1996.

AMTD
7, 6501–6528, 2014

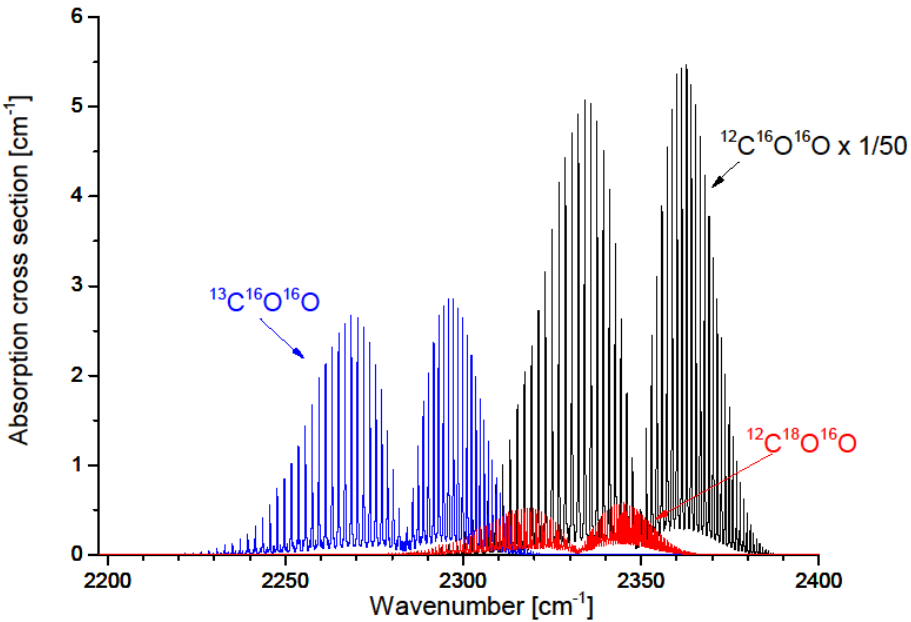

Figure 1. Absorption cross section for natural abundances of $^{12}C^{16}O^{16}O$, $^{13}C^{16}O^{16}O$ and $^{12}C^{16}O^{18}O$ in air computed with MALT from HITRAN (T = 303 K, p = 1 atm, app. resolution = 1 cm^{-1}, optical pathway = 24 m). The cross-section for $^{12}C^{16}O^{16}O$ is scaled down by a factor of 50.

AMTD
7, 6501–6528, 2014

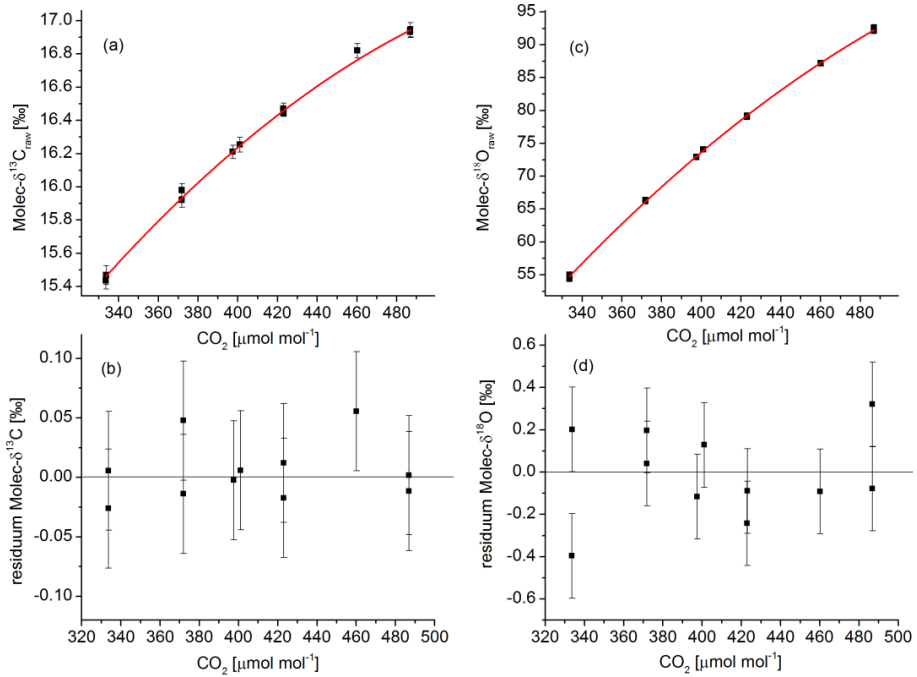

Figure 2. CO_2 dependence of raw Molec-δ^{13}C and Molec-δ^{18}O **(a)** and **(c)** and their residuals from the cubic fit **(b)** and **(d)**. The experimental results shown here were obtained in August 2012; the same experiment was performed in March 2014 and showed no significant difference to the earlier measurements.

AMTD
7, 6501–6528, 2014

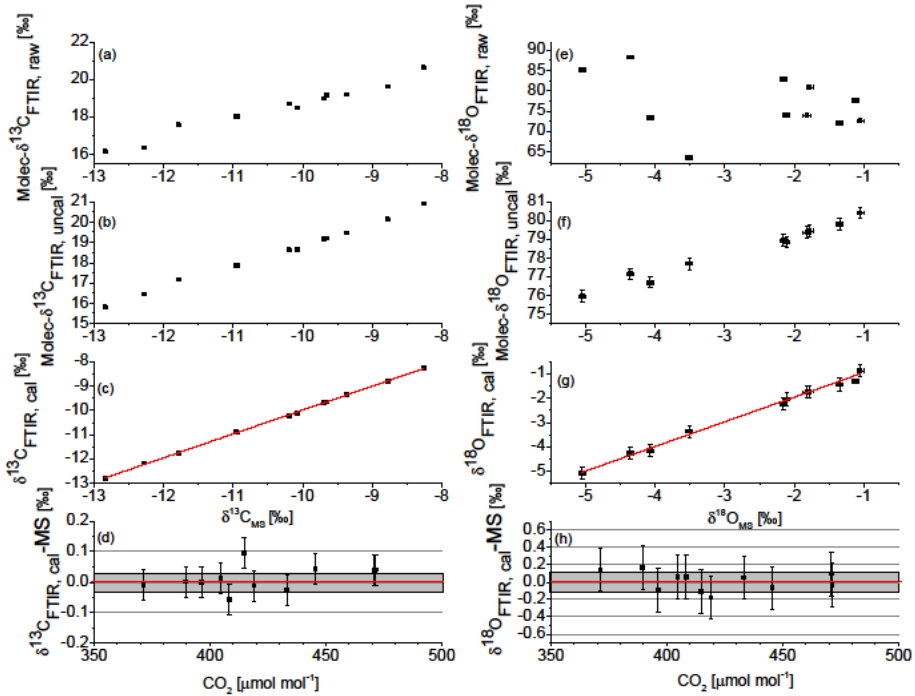

Figure 3. (a) Raw, **(b)** cross- and interspecies corrected (but still un-calibrated) and **(c)** calibrated δ^{13}C measurements and **(e)** raw, **(f)** cross- and interspecies corrected (but still un-calibrated) **(g)** calibrated δ^{18}O measurements of different target cylinders against the mass-spectrometric measurement of the same cylinders. Lowest panels: **(d)** Calibrated FTIR δ^{13}C value minus reference value measured by the Heidelberg mass spectrometer, **(h)** same as **(d)** for δ^{18}O, both plotted vs. the CO_2 mole fraction of the samples. The red lines in the lowest panels give the mean difference between the FTIR-measured values and the mass spectrometer and the grey areas show the standard deviation of the differences.

AMTD
7, 6501–6528, 2014

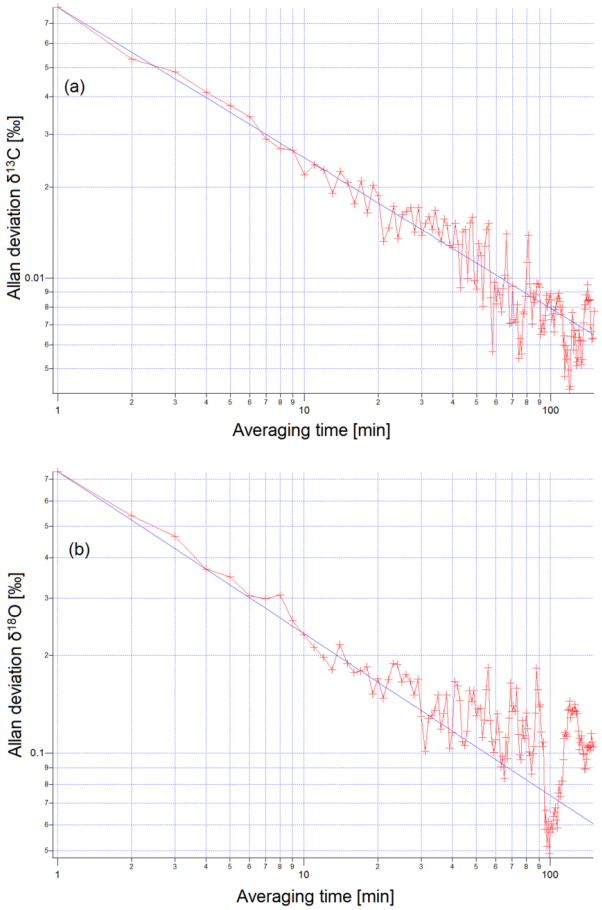

Figure 4. Allan deviation of **(a)** δ^{13}C-CO_2 and **(b)** δ^{18}O-CO_2 measured on the 5/6 August 2013 with the FTIR.

AMTD
7, 6501–6528, 2014

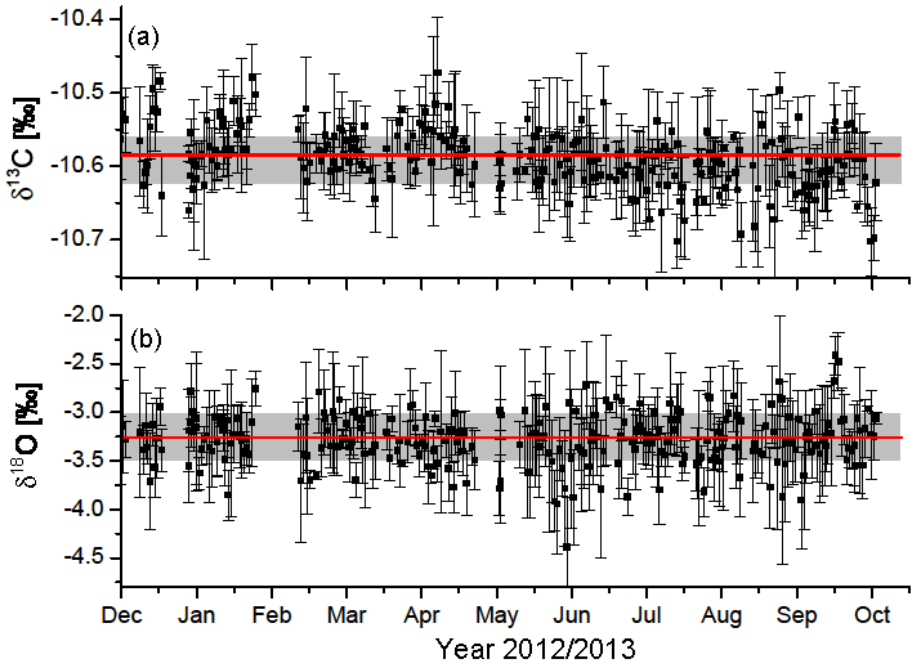

Figure 5. Repeated daily working gas measurements (9 min averages) depict a reproducibility of ±0.04 ‰ for δ^{13}C **(a)** and of ±0.27 ‰ for δ^{18}O **(b)** for the period from December 2012 to October 2013. Red lines: mean values, gray areas: standard deviation.

AMTD
7, 6501–6528, 2014

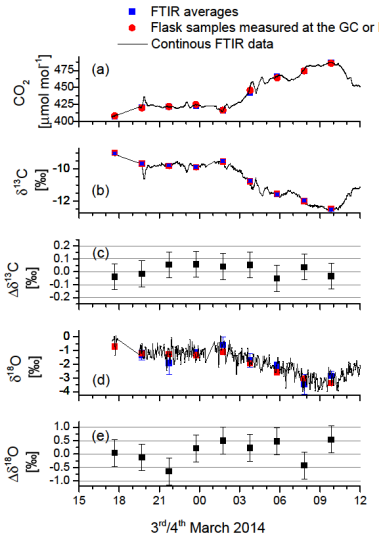

Figure 6. Diurnal cycle event sampled on the 3/4 March 2014 at the Institut für Umweltphysik in Heidelberg. Red: GC concentration (in case of CO_2) or mass spectrometric isotopologue value (in case of isotopologues) of flasks samples, blue: 9 minly averaged values from FTIR, black: continuous 3 min values from the FTIR, **(a)** CO_2 mole fraction, **(b)** δ^{13}C-CO_2 value **(c)** residual of 9-minuetly averaged FTIR δ^{13}C and mass spectrometric measurement (FTIR – mass spectrometer), **(d)** δ^{18}O-CO_2 value, **(e)** residual of 9-minuetly averaged FTIR δ^{18}O and mass spectrometric measurement (FTIR – mass spectrometer). All error bars on the (blue) averaged FTIR data are the standard deviation during the 9 min of averaging time. The error bars on the (red) mass spectrometric values show the typical reproducibility of our mass spectrometric measurements. The residual (FTIR-MS) has an error bar which combines the mass spectrometric and the FTIR uncertainties. In general, the FTIR reproduces the mass spectrometric values very well. The uncertainty given here combines the variability of atmospheric signal during the flask filling time as well as the reproducibility of the mass spectrometer and the FTIR measurements.

AMTD
7, 6501–6528, 2014

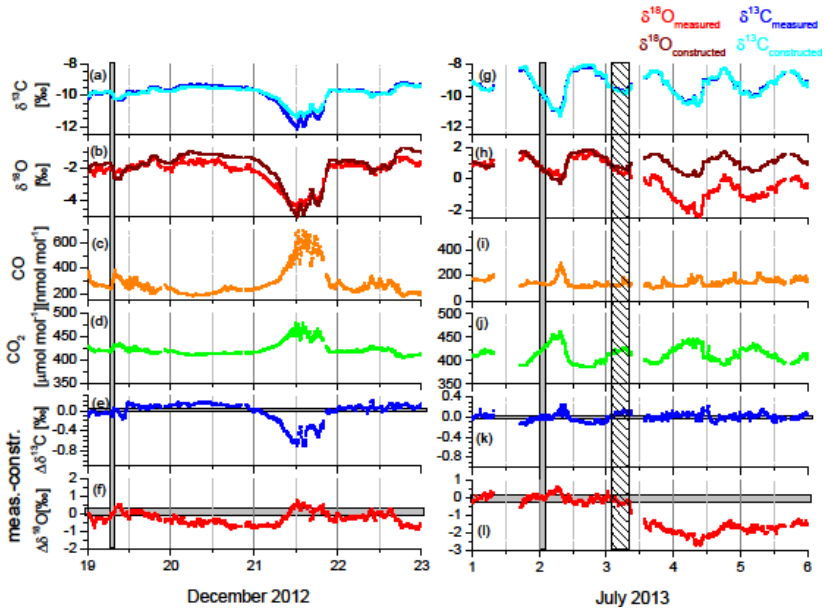

Figure 7. Trace gas records in winter (left panel) and summer (right panel) in Heidelberg. **(a)** and **(g)** show the measured (dark blue) and artificially constructed (light blue) δ^{13}C value, **(b)** and **(h)** the measured (red) and artificially constructed (burgundy) δ^{18}O value, **(c)** and **(i)** the measured CO value, **(d)** and **(j)** the measured CO_2 value. Panels **(e)** and **(k)** give the difference between the measured and constructed δ^{13}C value with a mean isotopic signature of $\delta^{13}C \approx -25$ ‰ in the wintertime and $\delta^{13}C \approx -27$ ‰ in the summer time. **(f)** and **(l)** give the difference between the measured and constructed δ^{18}O value with a mean isotopic signature of $\delta^{18}O_{VPDB} \approx -28$ ‰ in the wintertime and $\delta^{18}O_{VPDB} \approx -12$ ‰ in the summer time. Gray vertical bars indicate the "reference periods", in which the isotopic signature for artificially constructed δ^{13}C and δ^{18}O was determined. The dashed vertical bar in the right panel shows a period of high precipitation. Gray horizontal bars in **(f)** and **(l)** mark the 1σ-uncertainty of the isotope measurements.

AMTD
7, 6501–6528, 2014